Confinement Effects on the Nuclear Spin Isomer Conversion of H 2 O

Pierre-Alexandre Turgeon, Jonathan Vermette, Gil Alexandrowicz, Yoann Peperstraete, Laurent Philippe, Mathieu Bertin, Jean-Hugues Fillion, Xavier Michaut, Patrick Ayotte

Confinement Effects on the Nuclear Spin Isomer Conversion of H_2O

Pierre-Alexandre Turgeon,[†] Jonathan Vermette,[†] Gil Alexandrowicz,[‡] Yoann Peperstraete,[¶] Laurent Philippe,[¶] Mathieu Bertin,[¶] Jean-Hugues Fillion,[¶] Xavier Michaut,[*,¶] and Patrick Ayotte[*,†]

[†]*Département de chimie, Université de Sherbrooke, Sherbrooke, J1K 2R1, CANADA*

[‡]*Schulich Faculty of Chemistry, Technion - Israel Institute of Technology, Technion City, Haifa 32000, ISRAEL*

[¶]*LERMA, Observatoire de Paris, PSL Research University, CNRS, Sorbonne Universités, UPMC Univ. Paris 06, F-75252 Paris, FRANCE*

E-mail: XavierMichaut, Tel.:33(0)144274474, Email:xavier.michaut@upmc.fr; PatrickAyotte, Tel.:819-821-8000, Email:patrick.ayotte@usherbrooke.ca

Abstract

The mechanism for interconversion between the nuclear spin isomers (NSI) of H_2O remains shrouded in uncertainties. The temperature dependence displayed by NSI interconversion rates for H_2O isolated in an Argon matrix provides evidence that confinement effects are responsible for the dramatic increase in their kinetics with respect to the gas phase, providing new pathways for o-H_2O↔p-H_2O conversion in endohedral compounds. This reveals intramolecular aspects of the interconversion mechanism which may improve methodologies for the separation and storage of NSI en route to application ranging from magnetic resonance spectroscopy and imaging to interpretations of spin temperatures in the interstellar medium.

Introduction

Collections of molecules that display indiscernible spin-bearing nuclei behave as a mixtures of nuclear spin isomers (NSI). While at high temperatures, their relative abundance is dictated by nuclear spin statistics, the occurrence of the different NSI at low temperatures is controlled by a complex interplay of symmetry considerations, quantum states degeneracies and energetics in addition to their interconversion kinetics (i.e., sample thermal history). In hydrogen gas, NSI interconversion is sufficiently slow to allow their separation and storage allowing subsequent manipulations. Consequently, several methodologies are nowadays available for the preparation of molecular hydrogen samples highly enriched in either of its NSI,[1,2] thereby enabling powerful magnetic resonance applications.[3] However, the case of polyatomic molecules still presents significant challenges. While only very slight enrichments have thus so far been reported for simple molecules (i.e., CH_3F, C_2H_4, H_2CO) using laser-based methods[4–6] much larger enrichments were reported for H_2O using molecular beam[7–9] or chromatographic methodologies.[10] Nevertheless, the paucity of general and efficient enrichment methodologies for the preparation of out-of-equilibrium spin populations in polyatomic molecules continues to hamper studies of their NSI interconversion mechanism

and rates. Conversely, improving our understanding of NSI interconversion is required to devise efficient separation and storage strategies hence, significant gaps still remain in our description of these important fundamental, and intimately intertwined processes.

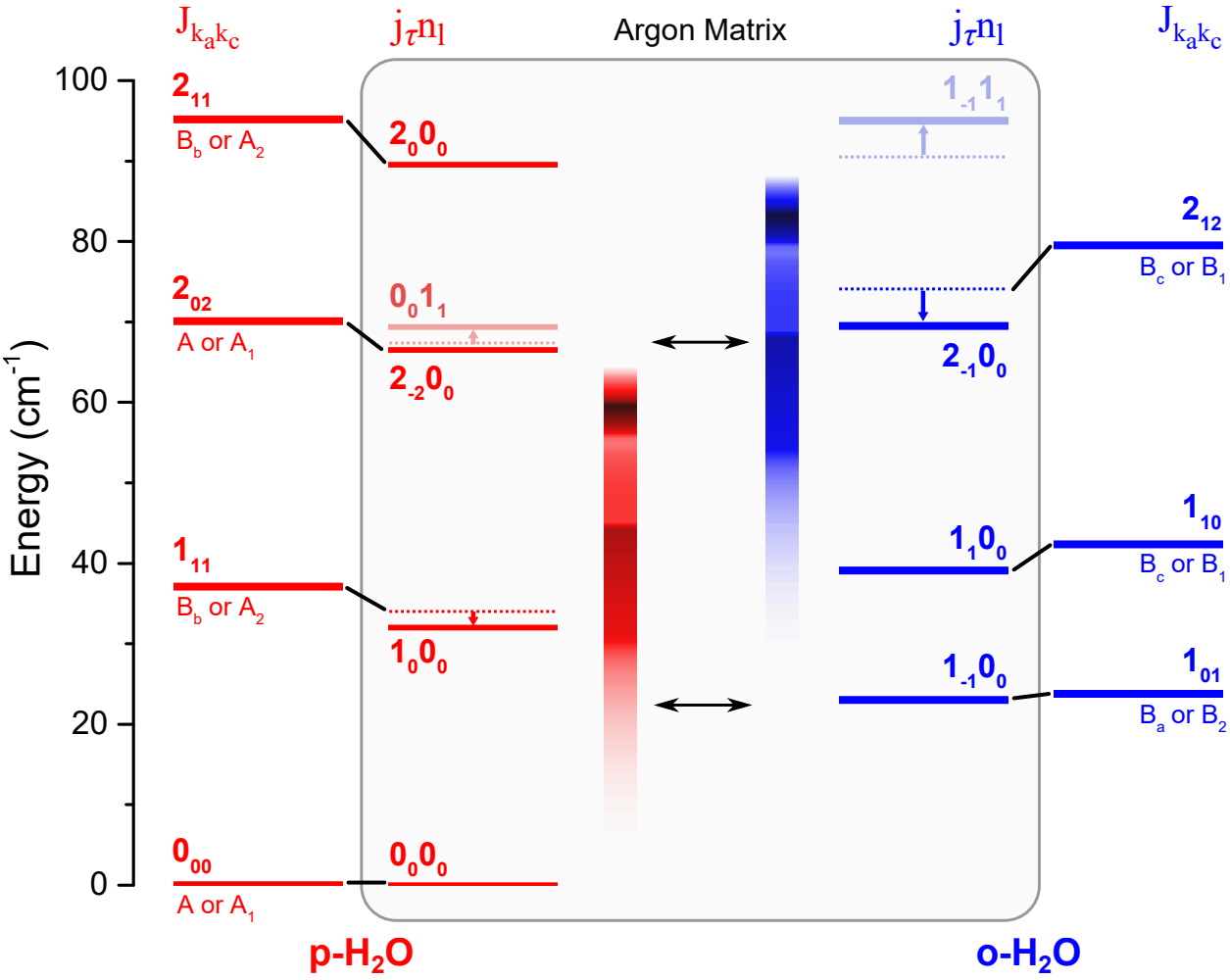

Figure 1: Energy levels diagram of gas phase H_2O[11] (far left and right) and H_2O@Ar[12] (shaded region). The gas phase states are labeled using the asymmetric rotor convention $J_{k_a k_c}$ while the confined states are identified using the quantum numbers of an asymmetric rotor j and τ, where $\tau = k_a - k_c$, and those of a 3D isotropic harmonic oscillator n and l. The double-headed arrows depict the NSI interconversion pathways highlighted in the present work. The phonon density of state of the argon crystal is displayed using vertical shaded bars alongside the o-H_2O@Ar and p-H_2O@Ar confined rotor energy levels (ref.[13,14]).

In isolated water molecules, the total nuclear spin is ever so weakly coupled to the other molecular degrees of freedom resulting in that, for most practical purposes, interconversion between ortho-H_2O (i.e., o-H_2O, whose rotational energy level are labeled using the conven-

tional approximate quantum numbers $J_{k_a k_c}$, and displayed to the far right of Figure 1) and para-H_2O (i.e., p-H_2O, Figure 1; far left) can often be considered as a forbidden process. Even in the absence of a spin conversion catalyst,[15] NSI interconversion may nonetheless arise in water vapour, albeit at a very slow rate, due to intermixing of very nearly degenerate o-H_2O and p-H_2O states[16,17] that couple through weak hyperfine interactions.[18] Incidentally, the coherence that may thus build between these weakly coupled states is eventually destroyed by external perturbations (i.e., intermolecular collisions), thereby causing the wavefunction of the mixed states to collapse and NSI interconversion to occur.[16,17] However, due to the magnitude of the intramolecular magnetic interactions (i.e., the spin-spin and spin-rotation coupling strengths are only on the order of a few tens of kHz),[19,20] this so-called "quantum relaxation" mechanism should only be operative at elevated temperatures (where nearly degenerate, highly rotationally excited states acquire significant population)[16,17] and pressures (thereby increasing the rate of intermolecular collisions).[21]

Furthermore, while it can be easily shown that the dipole-dipole interaction between the protons' nuclear spins cannot couple o-H_2O and p-H_2O states, symmetry considerations impose strict selection rules upon which states can be coupled by the other intramolecular magnetic interactions within the H_2O molecule.[16] Indeed, the spin-rotation (SR) Hamiltonian (which transforms as B_1 in the C_{2v} point group)[16] can only couple rotational states of certain symmetries, namely $A_1 \leftrightarrow B_1$ and $A_2 \leftrightarrow B_2$. Consequently, at very low temperatures, ever so small contributions to the NSI interconversion rate by ways of the SR coupling are only to be expected between the 1_{01} o-H_2O state and the 1_{11} (as well as 2_{11}) p-H_2O state while, at slightly higher temperatures, conversion may be mediated by SR couplings between the 2_{02} p-H_2O state and the 1_{10} (as well as 2_{12}) o-H_2O state. Interestingly, symmetry considerations forbid the coupling of any o-H_2O state with the 0_{00} ground state of p-H_2O by ways of the SR interaction. Therefore, given our current grasp of the mechanism for NSI interconversion, it is thus widely believed that, under the cold and dilute conditions of the interstellar medium, the NSI lifetimes for isolated H_2O molecules could reach billions of years.[22]

NSI interconversion in H_2O was reported to proceed at a much greater rate in the condensed phase (i.e., inert matrices, liquid water, amorphous or crystalline ice),[23–26] possibly mediated by inter-molecular spin-spin (SS) couplings.[27,28] However, there has also been some reports of highly stable out-of-equilibrium spin state populations in liquid water and in crystalline ice.[10] While at odds with the rapid NSI interconversion promoted by the inter-molecular SS coupling, these claims supported an intriguing proposition from the astrophysical community, namely that the unexpectedly low spin "temperatures" in comas[29,30] and protoplanetary disks[31] could be vestiges of the conditions of formation of these celestial icy bodies and/or of their constitutive molecular material, thereby providing a valuable "astronomical clock".[32] This hypothesis raises the interesting question of how the populations of H_2O spin states in ice are related to those of the adsorbing/desorbing water molecules.[32–35] Clearly, a better understanding of the (intra- and inter-molecular) NSI interconversion mechanisms and rates is required in order to improve the interpretation of astrophysical proxies while it may also contribute to develop better methodologies for the separation[7,9] and storage[8] of o-H_2O, opening up prospects for orders of magnitude enhancements in sensitivity for magnetic resonance spectroscopy and imaging.[3,7]

Experimental Section

Confinement effects on the NSI interconversion mechanism and rates for matrix isolated H_2O@Ar were examined by scrutinizing the o-H_2O↔p-H_2O interconversion kinetics at temperatures between 4K and 25K using infrared spectroscopy. Matrix isolated H_2O, a well-known[23] class of endohedral H_2O compounds along with $H_2O@C_{60}$,[36,37] was prepared by slowly condensing a mixture of water vapor and argon gas onto a gold-plated copper substrate at 20K. These conditions are known to result in H_2O molecules being confined to substitutional sites in a crystalline rare gas matrix.[38–40] Under our experimental conditions, argon has been shown to adopt a Face-Centered Cubic (FCC, which displays O_h symme-

try substitutional site) crystal structure while the occurrence of the metastable Hexagonal Close-Pack (HCP, which displays D_{3h} symmetry substitutional site) crystal structure may be promoted by impurities.[41] In contrast to CH_4@Ar,[42] where distinctive spectral features (i.e., the crystal field splitting of spectral features due to the degeneracy of the rovibrational sublevels being lifted in the D_{3h} symmetry HCP sites) and different NSI interconversion kinetics could be attributed to molecules trapped in HCP and FCC sites, neither could be observed in H_2O@Ar.[23–25] At a dilution ratio of 1 H_2O:1000 Ar, contributions from inter-molecular couplings[27,28] to the NSI interconversion rates of H_2O have been shown to be negligible[24,25] allowing intra-molecular contributions to be highlighted.

Results and Discussion

The shaded region in Figure 1 displays the rotational-translational (RT) energy levels for H_2O@Ar,[12] which were also calculated by Ceponkus et al,[43] according to the toy model originally proposed by Friedman and Kimmel.[44] While it reveals that H_2O molecules rotate relatively "unhindered", confinement of H_2O to a substitutional site of a rare gas matrix has three important consequences. Firstly, rotational motion of the H_2O molecule does not proceed around its center-of-mass (COM), but rather around its center-of-interaction (COI) with the Ar matrix. The energy level diagram for the confined quantum asymmetric rotor can thus be most simply interpreted using effective rotational constants A and C for H_2O@Ar that are significantly smaller than those of free H_2O (effective confined rotor states are linked to their corresponding free rotor states in Figure 1). This simple model allows one to estimate that the COI is located (0,15±0.01 Å) away from the COM of H_2O and that it lies along its C_2-axis. Secondly, H_2O@Ar displays local oscillator (LO) states (reported in Figure 1 as lighter shaded levels near 68 cm^{-1} for p-H_2O@Ar and near 95 cm^{-1} for o-H_2O@Ar) resulting from quantization of the frustrated translational motions of H_2O confined to interstitial sites in the Ar crystal.[45] Finally, rotation around the COI results in a strong coupling between

rotational and (frustrated) translational motion of confined H_2O@Ar. Despite evidence[39,46,47] for significant RT coupling in H_2O@Ar, confined rotor states are nonetheless labeled using the (uncoupled) asymmetric rotor quantum numbers j and τ, and the isotropic 3-D harmonic oscillator quantum numbers n and l (i.e., $j_\tau n_l$) for convenience. An important consequence of confinement, as it relates to NSI interconversion, is therefore, the strong mixing, and thus repulsion, between the $1_0 0_0$ (rotational) and $0_0 1_1$ (LO) states of p-H_2O@Ar, and between the $2_{-1} 0_0$ (rotational) and $1_{-1} 1_1$ (LO) states of o-H_2O@Ar, as a result of the RT coupling.

Due to the quasi-free rotor character of H_2O@Ar, it is straightforward to probe their nuclear spin state populations using ro-vibrational spectroscopy.[23–26] This is illustrated in the inset to Figure 2, which reports the temporal evolution of the intramolecular HOH bending vibration (i.e., ν_2 mode) infrared spectral range of H_2O@Ar following a sudden decrease in sample temperature (T = 20K $\rightarrow$ 6K, at t = 0). The intensity of the transitions assigned to o-H_2O decreases, while that assigned to p-H_2O increases, as a result of NSI interconversion throughout the 45h duration the NSI interconversion kinetics were monitored at T = 6K. The relative oscillator strengths for the ro-vibrational transitions arising from both NSI were evaluated[24,25,47] allowing the time evolution of their relative abundances to be quantified as reported in Figure 2 for T = 6K (o-H_2O - open squares ; p-H_2O - open circles).

Assuming o-$H_2O \leftrightarrow$p-H_2O interconversion proceeds through reversible first-order kinetics (Figure 2, continuous lines), the effective interconversion rate constant (k_{eff}; Figure 3A), as well as the equilibrium constant (expressed as the asymptotic ortho-to-para ratio as t$\rightarrow \infty$, or OPR; Figure 3B), were obtained at several temperatures from 4K and up to 25K. Figure 3A shows that k_{eff} displays a weak temperature dependence up to $\sim$10K, but that it increases rapidly thereafter (until reliable rate constants could no longer be obtained at T>25K due to poor signal-to-noise ratio and increasingly rapid NSI interconversion).

Phonons of the Ar matrix, whose density of states is indicated as vertical shaded bars in Figure 1,[13,14] play an important role in the NSI interconversion mechanism which can be described rather well by empirical spin-lattice relaxation models (Figure 3A, continu-

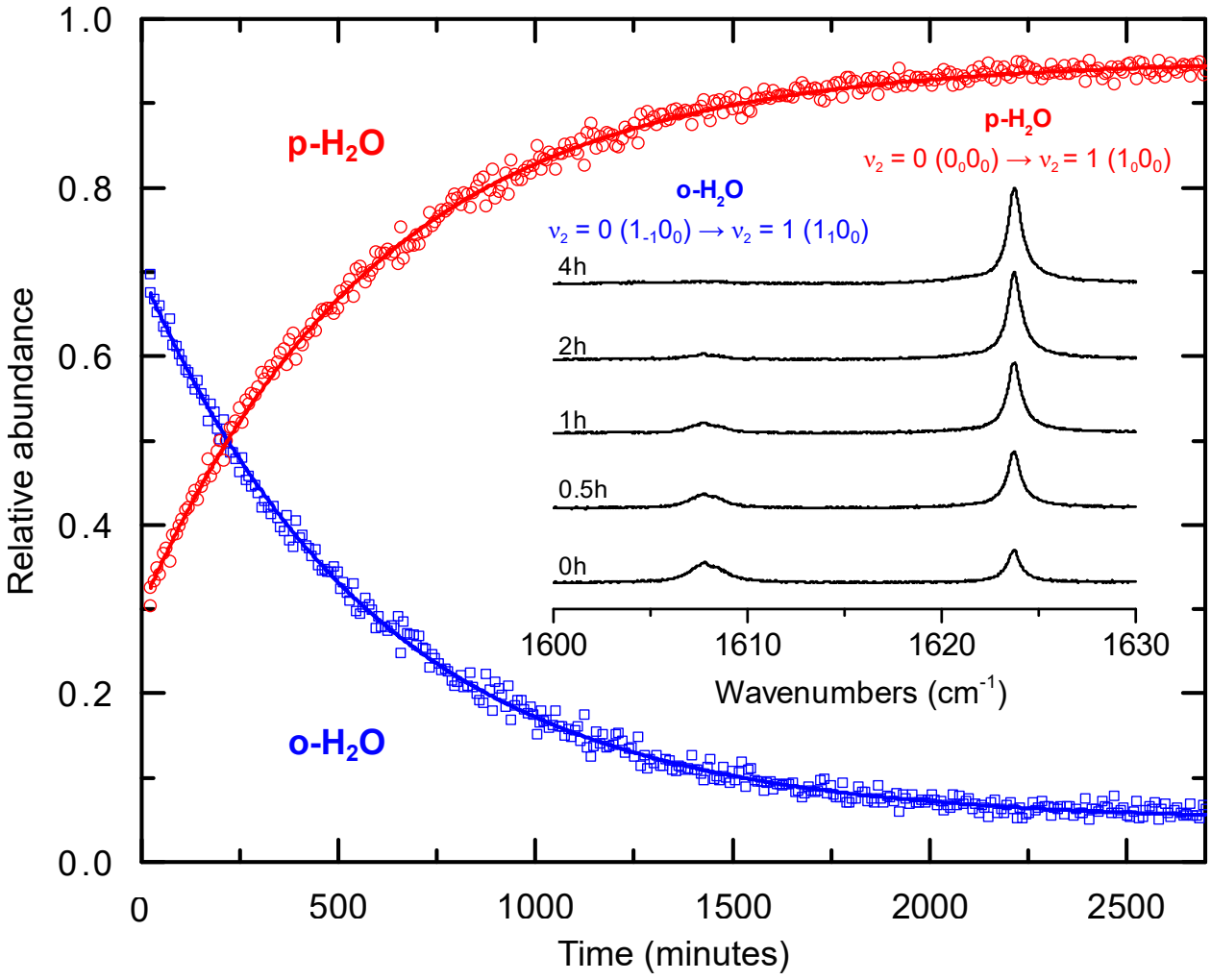

Figure 2: NSI interconversion of H_2O@Ar at 6K causes ortho-H_2O (open-squares) to convert to para-H_2O (open-circles) and the OPR to decay from ~1.7 to <0.1. The red and blue lines show the excellent agreement with a reversible first-order kinetics model.

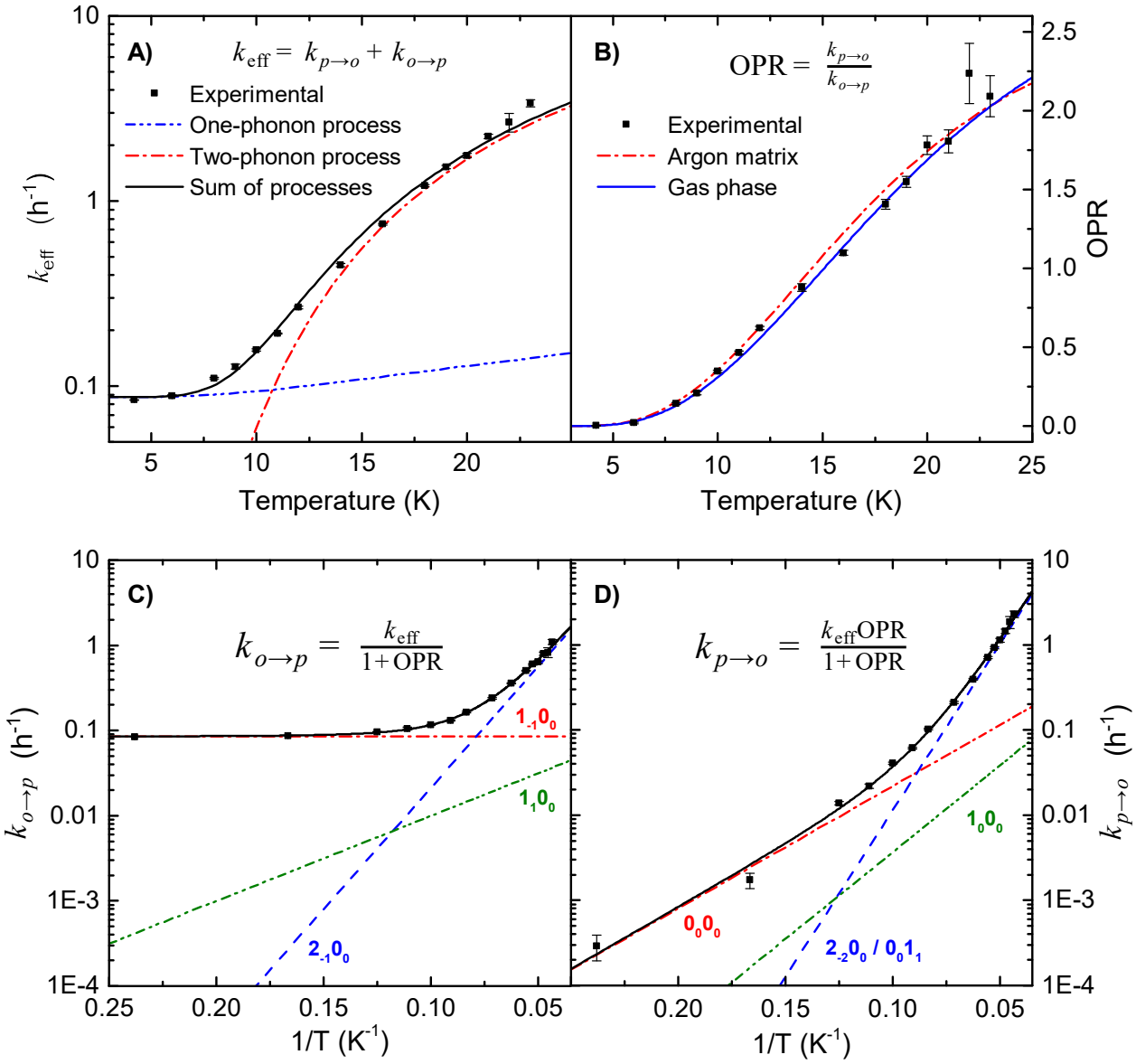

Figure 3: (A) The experimental effective first-order rate constants (black squares) are compared to the empirical spin-lattice models proposed in ref.[48] (B) The experimentally measured OPRs (black squares), which agree with the gas phase OPR[a] and the calculated OPR for H_2O@Ar[b], allowed the calculation of the reversible rate constants $k_{o\to p}$ (C) and $k_{p\to o}$ (D) from k_{eff} (A) assuming interconversion proceeds by reversible first-order kinetics. Individual contributions from specific RT levels to the interconverison rate could thus be deduced exclusively from experimental data.

[a]OPR for H_2O were calculated using the most recent IUPAC data.[11]

[b]OPR was calculated for H_2O@Ar using the energy levels from ref.,[12] displayed in Figure 1, which summarizes results from FIR and MIR spectroscopies, as well as INS (Ref[24,25,38–40,43]).

ous line).[26,48–50] At T<10K, the contribution from a reversible one-phonon process [i.e., the so-called "direct process" o-H_2O↔p-H_2O+$\hbar\omega_{Ar}$, whose temperature behavior scales as $\coth(\hbar\omega_{Ar}/2RT)$ with $\hbar\omega_{Ar} \sim 23$ cm^{-1}] appears to dominate NSI interconversion rates (Figure 3A, blue dash-dot-dot line). At T>10K, contributions from reversible two-phonons processes, o-H_2O+$\hbar\omega'_{Ar}$ ↔ p-H_2O+$\hbar\omega''_{Ar}$, to the NSI interconversion rates become increasingly important. While the temperature dependence of the experimental data is coherent with a resonant two-phonons Orbach process [i.e., which scales as $\exp(-\Delta/RT)$ with $\Delta \sim 46$cm^{-1}] (Figure 3A, red dash-dot line), a contribution from the non-resonant two-phonons Raman process [which scales as T^n, with $n \sim 7$, and showed to be dominant in case of H_2 adsorbed onto Amorphous Solid Water[50]] cannot be ruled out [and is even expected at higher temperatures which would, hence, better describe the temperature dependence of the conversion rate for T>20K]. Finally, the temperature dependence displayed by the spectroscopically determined OPR (Figure 3B - full square) agrees quite well with that calculated, using the energy level diagrams of Figure 1, for gas-phase H_2O (continuous line)[11] and for confined H_2O@Ar (dashed line).[12,43]

Pressing on within the assumption that NSI interconversion proceeds through reversible first-order kinetics and exploiting detailed balance, the first-order rate constants for the o-H_2O→p-H_2O ($k_{o\to p}$) and p-H_2O→o-H_2O ($k_{p\to o}$) unimolecular first-order half-reactions were calculated from the experimentally determined k_{eff} (Figure 3A) and OPR (Figure 3B). The Arrhenius plots for $k_{o\to p}$ (Figure 3C) and $k_{p\to o}$ (Figure 3D) reveal clearly that the NSI interconversion kinetics in H_2O@Ar display two distinct temperature regimes. For temperatures below about 10K (i.e., $T^{-1} > 0.1$), the o-H_2O→p-H_2O half-reaction (Figure 3C) appears barrier-less ($E^{o\to p}_{a,\text{low }T} = 0.6 \pm 0.3$cm^{-1}), whereas the p-$H_2O$→o-$H_2O$ half-reaction (Figure 3D) displays an apparent activation energy, $E^{p\to o}_{a,\text{low }T} = 22\pm2$ cm^{-1}. Above about 10K (i.e., $T^{-1} < 0.1$), the o-H_2O→p-H_2O (Figure 3C) and p-H_2O→o-H_2O (Figure 3D) half-reactions display apparent activation energies $E^{o\to p}_{a,\text{high }T} = 46 \pm 2$ cm^{-1} and $E^{p\to o}_{a,\text{high }T} = 58 \pm 4$ cm^{-1}, respectively. These apparent activation energies are displayed as double-headed arrows on

the energy diagram for H_2O@Ar in Figure 1.

In the spirit of the "quantum relaxation" model,[16,17] this may help pinpoint the gateway RT states that mediate NSI interconversion in H_2O@Ar thereby providing invaluable insight into the underlying mechanism. Accordingly, the empirical rate constants $k_{o\to p}$ (Figure 3C) and $k_{p\to o}$ (Figure 3D) were described by a sum of Boltzmann-weighted contributions from individual RT states (Figure 1).[16] This allows to determine that, at T>10K, interconversion proceeds mostly through coupling between the $2_{-1}0_0$ RT state of o-H_2O and the $2_{-2}0_0/0_01_1$ RT states of p-H_2O and that their contributions to the o-H_2O→p-H_2O and p-H_2O→o-H_2O rates are (13.0 ± 0.2) h^{-1} and (85 ± 30) h^{-1}, respectively. Here, confinement effects manifest themselves most prominently through the strong RT coupling between confined o-H_2O states which display the same total angular momentum $J = j + l = 2$,[43] namely the $2_{-1}0_0$ (mostly rotational) and $1_{-1}1_1$ (mostly LO) states of o-H_2O. As a result, the $2_{-1}0_0$ o-H_2O state acquires LO character and is significantly stabilized whereby it becomes close enough in energy to the 0_01_1 (LO) and $2_{-2}0_0$ (rotational) states of p-H_2O@Ar to allow interactions through the weak spin-rotation coupling thereby enhancing NSI interconversion. This interpretation is currently being validated using isotope substitution ($H_2{}^AO$, A=16,17,18) and different confining medium (Ne, Ar, Kr, Xe) allowing to systematically tune the rotational energy levels of H_2O@Ar and to modulate the strength of the RT coupling. Nonetheless, additional contributions arising from naturally occurring magnetic isotopes (^{21}Ne, ^{83}Kr, ^{129}Xe, ^{131}Xe, ^{17}O) need to be accounted for since they open new intermolecular NSI interconversion pathways.

The most intriguing finding reported herein remains, however, the unexpectedly rapid NSI interconversion observed at T<10K. Indeed, while interconversion at these temperatures is expected to be extremely inefficient in free H_2O due to the strongly forbidden character of the intramolecular SS and SR magnetic couplings between the 0_{00} p-H_2O and 1_{01} o-H_2O ground states,[22] comparatively large rates are observed in H_2O@Ar. Furthermore, the weak temperature dependence displayed by k_{eff} at T<10K (Figure 3A) strongly suggests creation

and annihilation of $\hbar\omega \sim 23$ cm^{-1} phonons in the Ar matrix and their scattering with confined H_2O can promote NSI interconversion at an appreciable rate. The low temperature behaviors of k_{eff} and OPR allow the contributions to NSI interconversion from the direct mechanism (i.e., o-$H_2O \leftrightarrow$p-$H_2O+\hbar\omega_{\text{Ar}}$) to be estimated as (0.085 ± 0.003) h^{-1} from the $1_{-1}0_0$ o-H_2O ground state and (0.6 ± 0.1) h^{-1} from the 0_00_0 p-H_2O ground state[1]. Here, confinement effects must allow to overcome the strongly forbidden character of the hyperfine SS and SR couplings to the p-H_2O ground state. This might arise from the mixing between RT states of the C_{2v} asymmetric quantum rotor due to trapping in the O_h crystal field of cuboctaedral geometry of an argon matrix substitutional site. Indeed, Momose and coworkers previously explored crystal field effect as they pertained to the NSI interconversion kinetics displayed by CD_4/CH_4@p-H_2.[49] They also invoked magnetic interactions of higher orders than spin-spin or spin-rotation couplings which remain highly forbidden for methane in p-H_2 matrices. The situation, however, is significantly more complex in H_2O@Ar due to couplings between angular momenta for intramolecular rotation, orbital motion of the 3D harmonic oscillator, and the precession of the water molecules' center of mass around the cavity. Therefore, in addition to phonon scattering, these intricate angular momentum coupling schemes arising from quantum confinement effects in H_2O@Ar must open novel NSI interconversion pathways that do not exist in free H_2O.

Proper account for these confinement effects on the complex coupled rotational-translational motions in H_2O@Ar would require solving the full dimensional Hamiltonian for the confined asymmetric rotor. This was achieved for CO@C_{60} by Olthof et al.,[51] for H_2O@C_{60} by Felker and Bačić[52] as well as for H_2@C_{60}, HD@C_{60} and D_2@C_{60} by Xu et al.[53] These studies described how the rotation of the "incarcerated" molecule results in a very strong coupling between the angular momenta of the rotating molecule and that arising from the rotation of its center of mass around the center of interaction within the cavity thus providing the

[1]Upper limits to the rate from the 1_10_0 o-H_2O state and from the 1_00_0 p-H_2O states are estimated to be (0.13 ± 0.06) h^{-1} and (0.7 ± 0.9) h^{-1} respectively, however, their contributions to the empirical rate constants is no more than 20%.

basis for strong RT coupling. In order to garner deeper insight into the effects of quantum confinement and its role in mediating new and alternate pathways for NSI interconversion in H_2O@Ar, the interaction potential between H_2O and the argon matrix was explored using accurate (high-level electronic structure-based[54] or spectroscopic[55]) Ar-H_2O pair potentials. As displayed in Figure 4, the most salient feature of this (only very slightly anisotropic) potential for H_2O@Ar is that the center-of-mass of the water molecule does not coincide with the geometric center of the cavity. As displayed in Figure 4A, the minimum energy configurations, in any given orientation of the water molecule, are found when the COM of H_2O recedes $\rho \approx 0.2$Å away from the geometric center of the cavity along its C_2 (i.e, rotational b) axis. Furthermore, the frequency of the (uncoupled 3-D harmonic) LO mode for H_2O@Ar was estimated to be $\omega_{LO} \approx 60$ cm^{-1}. These values are in reasonable agreement with those obtained by Ceponkus et al. (i.e., $\rho \approx 0.1$Å, and $\omega_{LO} \approx 68$ cm^{-1})[43] considering the simplicity of their model. The topology of the confining potential therefore possess characteristics that should result in much stronger mixing between the rotational and (frustrated) translational motions in H_2O@Ar than that reported, for example, for $H_2O@C_{60}$.[51] Furthermore, while inter-molecular coupling between H_2O and the stiff fullerene cage were neglected in $H_2O@C_{60}$, the role of the soft phonon modes in H_2O@Ar, which is responsible for the rapid thermalization of rotational motion and the efficient NSI interconversion, should be explicitly taken into account for a proper description of NSI interconversion in H_2O@Ar.

The temperature dependence of the effective first-order rate constant, k_{eff}, and equilibrium constant, OPR, enabled detailed analysis of which rotational-translation states contribute most to the interconversion mechanisms in H_2O@Ar. Confinement effects provide dramatic enhancements in the o-H_2O↔p-H_2O interconversion rates in argon matrices. Improving our understanding of confinement effect on the NSI interconversion mechanisms and rates should enable better storage strategies to be devised for water samples highly enriched in o-H_2O en route towards NMR applications to quantum information, spectroscopy and

imaging. It may also provide more robust interpretations of the nuclear spin isomer populations observed in the interstellar medium.

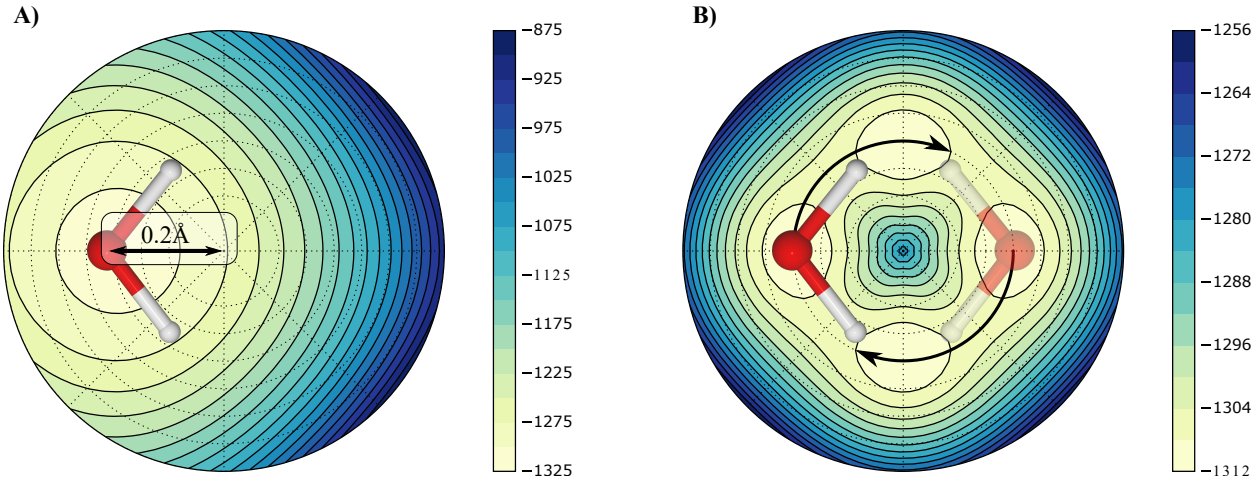

Figure 4: Potential energy surface (cm^{-1}) resulting from the interaction of an H_2O molecule with the 12 nearest neighbors of an Ar FCC crystal substitutional site. The potential was calculated using a pairwise interaction potential.[54,55] Calculations using an HCP structure reproduced the main features of the potential, displaying only subtle differences. Panel A) presents the interaction potential for a water molecule moving along the [100] plane with its orientation fixed with respect to the face-centered cubic argon crystal, thereby highlighting the nearly harmonic character of the confining potential. Panel B) presents the diabatic interaction potential for a water molecule moving in the same plane while maintaining an orientation where the C_2 axis points toward the center of the cavity (as a result of strong RT coupling).

Conclusion

NSI interconversion kinetics of H_2O isolated in argon matrices was scrutinized using rovibrationnal spectroscopy at low temperature. The strong confinement effects observed spectroscopically in H_2O@Ar were shown to partially lift the rigorous selection rules that govern spin conversion in individual molecules, specially the forbidden coupling between the ortho and para ground states. Given the unprecedented quality of the data presented herein, this work brings new light to the long-studied problem of ortho/para conversion in H_2O by providing quantitative contributions of individual rotational-translational levels to the effective conversion rate. As this works is the first to provide state specific kinetics at low temperature,

it constitutes a milestone in the elucidation of underlying NSI interconversion mechanisms.

Acknowledgement

Financial support by NSERC, CFI and CQMF is greatfully acknowledged. This work was supported by the French program funded by CNRS and CNES named "Physique et Chimie du Milieu Interstellaire" (PCMI) and the French National Research Agency (Project ANR GASOSPIN number 09-BLAN-0066-01). GA gratefully acknowledges funding from the German-Israeli Foundation for Scientific Research and the European Research Council under the European Unions seventh framework program (FP/2007-2013)/ERC grant 307267. PA gratefully acknowledges support by UPMC and CPCFQ during his sabbatical leave. Authors thank Karen Monneret and Julien Camperi for assistance.

References

(1) Farkas, A. *Orthohydrogen, parahydrogen and heavy hydrogen*; Cambridge series of physical chemistry; The University press, 1935.

(2) Fukutani, K.; Sugimoto, T. Physisorption and ortho-para conversion of molecular hydrogen on solid surfaces. *Prog. Surf. Sci.* **2013**, *88*, 279–348.

(3) Bowers, C. R.; Weitekamp, D. P. Transformation of symmetrization order to nuclear-spin magnetization by chemical reaction and nuclear magnetic resonance. *Phys. Rev. Lett.* **1986**, *57*, 2645–2648.

(4) Sun, Z.-D.; Takagi, K.; Matsushima, F. Separation and conversion dynamics of four nuclear spin isomers of ethylene. *Science* **2005**, *310*, 1938–1941.

(5) Nagels, B.; Schuurman, M.; Chapovsky, P.; Hermans, L. Nuclear spin conversion in

molecules: Experiments on CH^{13}_3F support a mixing-of-states model. *Phys. Rev. A* **1996**, *54*, 2050–2055.

(6) Peters, G.; Schramm, B. Nuclear spin state relaxation in formaldehyde: dependence of the rate constant on pressure. *Chem. Phys. Lett.* **1999**, *302*, 181–186.

(7) Kravchuk, T.; Reznikov, M.; Tichonov, P.; Avidor, N.; Meir, Y.; Bekkerman, a.; Alexandrowicz, G. A magnetically focused molecular beam of ortho-water. *Science* **2011**, *331*, 319–321.

(8) Turgeon, P.-A.; Ayotte, P.; Lisitsin, E.; Meir, Y.; Kravchuk, T.; Alexandrowicz, G. Preparation, isolation, storage, and spectroscopic characterization of water vapor enriched in the ortho-H_2O nuclear spin isomer. *Phys. Rev. A* **2012**, *86*, 062710.

(9) Horke, D. A.; Chang, Y.-P.; Długołęcki, K.; Küpper, J. Separating para and ortho water. *Angew. Chem.* **2014**, *53*, 11965–11968.

(10) Tikhonov, V. I.; Volkov, A. Separation of water into its ortho and para isomers. *Science* **2002**, *296*, 2363.

(11) Tennyson, J.; Bernath, P. F.; Brown, L. R.; Campargue, A.; Császár, A. G.; Daumont, L.; Gamache, R. R.; Hodges, J. T.; Naumenko, O. V.; Polyansky, O. L. et al. IUPAC critical evaluation of the rotational-vibrational spectra of water vapor, Part III: Energy levels and transition wavenumbers for H^{16}_2O. *J. Quant. Spectrosc. Radiat. Transfer* **2013**, *117*, 29–58.

(12) Perchard, J. Anharmonicity and hydrogen bonding. III. Analysis of the near infrared spectrum of water trapped in argon matrix. *Chem. Phys.* **2001**, *273*, 217–233.

(13) Fujii, Y.; Lurie, N. A.; Pynn, R.; Shirane, G. Inelastic neutron scattering from solid Ar^{36}. *Phys. Rev. B* **1974**, *10*, 3647–3659.

(14) Kaburaki, H.; Li, J.; Yip, S.; Kimizuka, H. Dynamical thermal conductivity of argon crystal. *Journal of Applied Physics* **2007**, *102*, 043514.

(15) Wigner, E. P. Über die paramagnetische Umwandlung von Para-Orthowasserstoff. III. *Z. Physik. Chem. B* **1933**, *23*, 28–32.

(16) Curl, R. F.; Kasper, J. V. V.; Pitzer, K. S. Nuclear spin state equilibration through nonmagnetic collisions. *J. Chem. Phys.* **1967**, *46*, 3220–3228.

(17) Chapovsky, P. L.; Hermans, L. J. F. Nuclear spin conversion in polyatomic molecules. *Annu. Rev. Phys. Chem.* **1999**, *50*, 315–345.

(18) Flygare, W. H. Magnetic interactions in molecules and an analysis of molecular electronic charge distribution from magnetic parameters. *Chem. Rev.* **1974**, *74*, 653–687.

(19) Cazzoli, G.; Puzzarini, C.; Harding, M. E.; Gauss, J. The hyperfine structure in the rotational spectrum of water: Lamb-dip technique and quantum-chemical calculations. *Chem. Phys. Lett.* **2009**, *473*, 21–25.

(20) Puzzarini, C.; Cazzoli, G.; Harding, M. E.; Vázquez, J.; Gauss, J. A new experimental absolute nuclear magnetic shielding scale for oxygen based on the rotational hyperfine structure of $H_2^{17}O$. *J. Chem. Phys.* **2009**, *131*, 234304.

(21) Cacciani, P.; Cosléou, J.; Khelkhal, M. Nuclear spin conversion in H_2O. *Phys. Rev. A* **2012**, *85*, 1–8.

(22) Tanaka, K.; Harada, K.; Oka, T. Ortho-para mixing hyperfine interaction in the H_2O^+ ion and nuclear spin equilibration. *J. Phys. Chem. A* **2013**, *117*, 9584–9592.

(23) Redington, R. L.; Milligan, D. E. Molecular rotation and ortho-para nuclear spin conversion of water suspended in solid Ar, Kr, and Xe. *J. Chem. Phys.* **1963**, *39*, 1276–1284.

(24) Pardanaud, C. Ph.D. thesis, Université Pierre et Marie Curie, 2007.

(25) Abouaf-Marguin, L.; Vasserot, A.-M.; Pardanaud, C.; Michaut, X. Nuclear spin conversion of H_2O trapped in solid xenon at 4.2K: A new assignment of ν_2 rovibrational lines. *Chem. Phys. Lett.* **2009**, *480*, 82–85.

(26) Fillion, J.-H.; Bertin, M.; Lekic, A.; Moudens, A.; Philippe, L.; Michaut, X. Understanding the relationship between gas and ice : experimental investigations on ortho-para ratios. *EAS Publications Series* **2012**, *58*, 307–314.

(27) Limbach, H.-H.; Buntkowsky, G.; Matthes, J.; Gründemann, S.; Pery, T.; Walaszek, B.; Chaudret, B. Novel insights into the mechanism of the ortho/para spin conversion of hydrogen pairs: implications for catalysis and interstellar water. *ChemPhysChem* **2006**, *7*, 551–554.

(28) Buntkowsky, G.; Limbach, H.-H.; Walaszek, B.; Adamczyk, A.; Xu, Y.; Breitzke, H.; Schweitzer, A.; Gutmann, T.; Wächtler, M.; Amadeu, N. et al. Mechanisms of dipolar ortho/para-H_2O conversion in ice. *Z. Phys. Chem.* **2008**, *222*, 1049–1063.

(29) Mumma, M. J.; Weaver, H. a.; Larson, H. P.; Davis, D. S.; Williams, M. Detection of water vapor in Halley's comet. *Science* **1986**, *232*, 1523–1528.

(30) Crovisier, J. The spectrum of comet Hale-Bopp (C/1995 O1) observed with the infrared space observatory at 2.9 astronomical units from the Sun. *Science* **1997**, *275*, 1904–1907.

(31) Hogerheijde, M. R.; Bergin, E. a.; Brinch, C.; Cleeves, L. I.; Fogel, J. K. J.; Blake, G.; Dominik, C.; Lis, D. C.; Melnick, G.; Neufeld, D. et al. Detection of the water reservoir in a forming planetary system. *Science* **2011**, *334*, 338–340.

(32) Hama, T.; Watanabe, N.; Kouchi, A.; Yokoyama, M. Spin temperature of water molecules desorbed from the surfaces of amorphous solid water, vapor-deposited and produced from photolysis of CH_4/O_2 solid mixture. *ApJ* **2011**, *738*, L15.

(33) Sliter, R.; Gish, M.; Vilesov, A. F. Fast nuclear spin conversion in water clusters and ices: A matrix isolation study. *J. Phys. Chem. A* **2011**, *115*, 9682–9688.

(34) Hama, T.; Watanabe, N. Surface processes on interstellar amorphous solid water: Adsorption, diffusion, tunneling reactions, and nuclear-spin conversion. *Chem. Rev.* **2013**, *113*, 8783–8839.

(35) Hama, T.; Kouchi, A.; Watanabe, N. Statistical ortho-to-para ratio of water desorbed from ice at 10 Kelvin. *Science* **2016**, *351*, 65–67.

(36) Kurotobi, K.; Murata, Y. A single molecule of water encapsulated in fullerene C_{60}. *Science* **2011**, *333*, 613–616.

(37) Beduz, C.; Carravetta, M.; Chen, J. Y.-C.; Concistre, M.; Denning, M.; Frunzi, M.; Horsewill, A. J.; Johannessen, O. G.; Lawler, R.; Lei, X. et al. Quantum rotation of ortho and para-water encapsulated in a fullerene cage. *Proc. Natl. Acad. Sci. U.S.A.* **2012**, *109*, 12894–12898.

(38) Langel, W.; Schuller, W.; Knözinger, E.; Fleger, H.-W.; Lauter, H. J. Disordered phases in vapor deposited rare gases. *J. Chem. Phys.* **1988**, *89*, 1741–1742.

(39) Knözinger, E.; Wittenbeck, R. Intermolecular motional degrees of freedom of water and water-d2 isolated in solid gas matrices. *J. Am. Chem. Soc.* **1983**, *105*, 2154–2158.

(40) Knözinger, E.; Schuller, W.; Langel, W. Structure and dynamics in pure and doped rare-gas matrices. *Faraday Discuss. Chem. Soc.* **1988**, *86*, 285–293.

(41) Meyer, L.; Barrett, C. S.; Haasen, P. New crystalline phase in solid argon and its solid solutions. *J. Chem. Phys.* **1964**, *40*, 2744.

(42) Jones, L.; Ekberg, S.; Swanson, B. Hindered rotation and site structure of methane trapped in rare-gas solids. *J. Chem. Phys.* **1986**, *85*, 3203–3210.

(43) Ceponkus, J.; Uvdal, P.; Nelander, B. The coupling between translation and rotation for monomeric water in noble gas matrices. *J. Chem. Phys.* **2013**, *138*, 244305.

(44) Friedmann, H.; Kimel, S. Rotation-translation coupling effect in noble gas crystals containing molecular impurities. *J. Chem. Phys.* **1967**, *47*, 3589–3605.

(45) Pitsevich, G.; Doroshenko, I.; Malevich, A.; Shalamberidze, E.; Sapeshko, V.; Pogorelov, V.; Pettersson, L. Temperature dependence of the intensity of the vibration-rotational absorption band $\nu 2$ of H_2O trapped in an argon matrix. *Spectrochimica Acta Part A: Molecular and Biomolecular Spectroscopy* **2017**, *172*, 83–90.

(46) Fry, H. A.; Jones, L. H.; Swanson, B. I. High-resolution spectra of the 1(1,1) 0(0,0) rotational transition of water in argon and krypton matrices. *Chem. Phys. Lett.* **1984**, *105*, 547–550.

(47) Michaut, X.; Vasserot, A.-M.; Abouaf-Marguin, L. Temperature and time effects on the rovibrational structure of fundamentals of H_2O trapped in solid argon: hindered rotation and RTC satellite. *Vib. Spectrosc.* **2004**, *34*, 83–93.

(48) Scott, P. L.; Jeffries, C. D. Spin-lattice relaxation in some rare-earth salts at Helium temperatures; observation of the phonon bottleneck. *Phys. Rev.* **1962**, *127*, 32–51.

(49) Miyamoto, Y.; Fushitani, M.; Ando, D.; Momose, T. Nuclear spin conversion of methane in solid parahydrogen. *J. Chem. Phys.* **2008**, *128*, 114502.

(50) Ueta, H.; Watanabe, N.; Hama, T.; Kouchi, A. Surface temperature dependence of hydrogen ortho-para conversion on amorphous solid water. *Phy. Rev. Lett.* **2016**, *116*, 253201.

(51) Olthof, E. H. T.; van der Avoird, A.; Wormer, P. E. S. Vibration and rotation of CO in C_{60} and predicted infrared spectrum. *J. Chem. Phys.* **1996**, *104*, 832–847.

(52) Felker, P. M.; Bačić, Z. Communication: Quantum six-dimensional calculations of the coupled translation-rotation eigenstates of $H_2O@C_{60}$. *J. Chem. Phys.* **2016**, *144*, 201101.

(53) Xu, M.; Sebastianelli, F.; Bačić, Z.; Lawler, R.; Turro, N. J. H_2, HD, and D_2 inside C_{60}: Coupled translation-rotation eigenstates of the endohedral molecules from quantum five-dimensional calculations. *J. Chem. Phys.* **2008**, *129*, 064313.

(54) Makarewicz, J. Ab initio intermolecular potential energy surfaces of the water-rare gas atom complexes. *J. Chem. Phys.* **2008**, *129*, 184310.

(55) Cohen, R. C.; Saykally, R. J. Multidimensional intermolecular dynamics from tunable far-infrared laser spectroscopy: Angular-radial coupling in the intermolecular potential of argon-H_2O. *J. Chem. Phys.* **1991**, *95*, 7891–7906.

Graphical TOC Entry